



UNICA

UNIVERSITÀ
DEGLI STUDI
DI CAGLIARI



Università di Cagliari

UNICA IRIS Institutional Research Information System

This is the Author's *accepted* manuscript version of the following contribution:

[SARA MARIA PANI, MARTA CIUFFI, MATTEO DEMURU, SIMONE MAURIZIO LA CAVA, GIOVANNI BAZZANO, ERNESTO D'ALOJA and MATTEO FRASCHINI, Subject, session and task effects on power, connectivity and network centrality: A source-based EEG study, Biomedical Signal Processing and Control, Volume 59, May 2020, 101891]

The publisher's version is available at:

<https://doi.org/10.1016/j.bspc.2020.101891>

When citing, please refer to the published version.

© <2020>. This manuscript version is made available under the CC-BY-NC-ND 4.0 license <https://creativecommons.org/licenses/by-nc-nd/4.0/>

This full text was downloaded from UNICA IRIS <https://iris.unica.it/>

Subject, session and task effects on power, connectivity and network centrality: a source-based EEG study

SARA MARIA PANI^{1*}, MARTA CIUFFI^{2*}, MATTEO DEMURU³, SIMONE MAURIZIO LA CAVA³, GIOVANNI BAZZANO², ERNESTO D'ALOJA² and MATTEO FRASCHINI³

¹Department of Biomedical Sciences, PhD Program in Neuroscience, University of Cagliari, I-09042, Italy

²Department of Medical Sciences and Public Health - Forensic Science Unit - University of Cagliari, Cagliari, Italy

³Department of Electrical and Electronic Engineering, University of Cagliari, Cagliari, I-09123, Italy

*Contributed equally to this work

Corresponding author: Matteo Fraschini (e-mail: fraschin@unica.it).

ABSTRACT

Inter-subjects' variability in functional brain networks has been extensively investigated in the last few years. In this context, unveiling subject-specific characteristics of EEG features may play an important role for both clinical (e.g., biomarkers) and bio-engineering purposes (e.g., biometric systems and brain computer interfaces). Nevertheless, the effects induced by multi-sessions and task-switching are not completely understood and considered. In this work, we aimed to investigate how the variability due to subject, session and task affects EEG power, connectivity and network features estimated using source-reconstructed EEG time-series. Our results point out a remarkable ability to identify stable subject features within a given task together with striking independence from the session. The results also show a relevant effect of task-switching, which is comparable to individual variability. This study suggests that power and connectivity EEG features may be adequate to detect stable (over-time) individual properties within predefined and controlled tasks and that these findings are consistent over a range of connectivity metrics, different epoch lengths and parcellation schemes.

Keywords: EEG, individuality, connectivity, task-switching

1. Introduction

During the last few years it has been further recognized and stressed the importance to highlight that individual variability may play a relevant role in human neuroimaging studies [1], [2]. The way in which each brain is unique and could be distinguished amidst a myriad of other brains is fascinating but unveiling the underlying subject-specific characteristics is crucial for both clinical (e.g., biomarkers) and bio-engineering purposes (e.g., biometric systems and brain computer interfaces). Recent studies have already highlighted the implications of individual variation for personalized approaches to mental illness [3], ADHD [4] and in the developing brain [5]. It has been also reported that these functional traits are familial, heritable and stable over a long time interval [6], [7]. Electroencephalographic (EEG) time-frequency [8] and connectivity-based [9]–[12] features have shown subject-specific characteristics comparable in terms of performance to other more common fingerprints.

Nevertheless, it has been recently shown that the performance of the connectivity-based biometric systems varies with the connectivity metric and with the specific task and is not yet investigated in terms of permanence (i.e., stability over-time) [13]. From this new perspective, with the clear evidence that functional brain networks vary across individuals, few studies investigated to what extent these subject-specific features are stable over time and over different states. Using functional Magnetic Resonance Imaging (fMRI), Gratton et al. [14] reported that functional networks are suited to detect stable individual characteristics with a limited contribution from task-state and day-to-day variability, thus suggesting their possible utility in the personalized medicine approach. Similarly, Cox et al. [15], using EEG scalp level analysis, have reported that, despite a shared structure is still discernible across individuals, well-defined subject-specific and stable over-time network profiles were clearly detectable.

In this study we aim to investigate if these subject-specific features are still detectable, stable over time and consistent among different tasks using an EEG source level approach. This approach should provide a more accurate description of the underlying network [16] since the connectivity estimates should be less prone to volume conduction and signal leakage problems. In order to investigate this question we analyzed source-reconstructed EEG time-series using three different and widely used analyses: Power Spectral Density (PSD), Phase Locking Value (PLV) [17] and nodal centrality network approaches, namely Eigenvector Centrality (EC). PSD has been shown to capture relevant subject-specific information [8] and represents a simple and easily interpretable EEG feature. PLV, in combination with weighted Minimum Norm Estimator (wMNE) [18], provides a good estimate of the functional brain organization in EEG [19] and, despite the PLV is not completely independent from the PSD [20], is

known to be affected by volume conduction and signal leakage, it still performs better than other common connectivity metrics in terms of subject authentication [13]. Moreover, as previously stated, the PLV was recently used at scalp-level to investigate the variability and the stability of large-scale cortical oscillation patterns [15]. Finally, it was reported that the EC, which captures more information about the network topology than straightforward measure such as the degree, represents a promising measure to design of EEG-based biometric systems [9]. The analysis was performed on a novel EEG dataset consisting of eleven healthy subjects, recorded over two different sessions (after four weeks) and performing four different tasks. All the codes are freely available in a Github repository at the following link: <https://github.com/matteogithub/individuality>.

2. Material and methods

2.1 Dataset

Fifteen healthy volunteers (7 females, mean age 31.9 ± 3.1 years, range 28 – 38) were enrolled in the present study. Informed consent was obtained prior to the recordings and the study was approved by the local ethics committee. EEG signals were recorded using a 61 channels EEG system (Brain QuickSystem, Micromed, Italy) during four different tasks and repeated over two different sessions (the second acquired four weeks later from the first). Recordings were acquired in a sitting position in a normal daylight room; a dimly lit and sound attenuated room and supine position were avoided to prevent drowsiness. Signals were digitized with a sampling frequency of 1024 Hz with the reference electrode placed in close approximation of the electrode POz. The four tasks consisted of: (T1) five minutes eyes-closed resting-state, (T2) five minutes eyes-open resting-state, (T3) two minutes eyes-closed simple mathematical task and (T4) two minutes eyes-closed complex mathematical task. During the simple mathematical task, the subjects were asked to perform multiple subtractions, while during the complex mathematical task, subjects were asked to perform a series two digits multiplications. Three subjects were excluded from the analysis due to low quality of the EEG recordings and another one missed the second session.

2.2 EEG preprocessing

All the preprocessing steps were performed using the freely available toolbox EEGLAB (version 13_6_5b) [21]. The raw EEG signals were re-reference to common average reference and band-pass filtered (with fir1 filter type) between 1 and 70 Hz and a notch filter set to 50 Hz was also applied. All the recordings were visually inspected and segments with clear artifacts were rejected and not further analyzed.

2.3 Source reconstruction

In order to obtain the source-reconstructed time-series, the Brainstorm software (version 3.4) [22] was used to compute the head model with a symmetric boundary element method in Open-MEEG [23] based on the anatomy derived from the ICBM152 brain (with 15,002 vertices) [24]. It has been recently shown that the co-registration performed with a template provided consistent relative power, connectivity, and network estimates compared to the use of the native MRI [25]. EEG time-series at source level were reconstructed using whitened and depth-weighted linear L2 minimum norm estimate (wMNE) [18], [26] and projected onto 68 regions of interest (ROIs) as defined by the Desikan-Killiany

atlas [27]. For more details about the atlas visualization, please refer to the following link:

<https://surfer.nmr.mgh.harvard.edu/fswiki/CorticalParcellation>

In order to investigate the possible effect of brain parcellation, the analysis was replicated using the Schaefer atlas with 17 networks as reported in [28]. All the steps were performed using the software Brainstorm [22].

2.4 Features extraction

After the EEG time-series were reconstructed at source level, in order to increase the quality of the analysis, for each subject, each task and each session, we selected the best (less contaminated) 10 EEG epochs (segments of 5 seconds) ordering all the available epochs on the basis of the three-sigma rule (consequently discarding segments presenting values over than 3 standard deviations from the mean) [29]. The analysis was also replicated using three different epoch length, respectively 6 s, 2 s and 1 s. Successively, for each selected epoch we have extracted three different features vectors, respectively for PSD, PLV and EC, representing the individual profiles or subject fingerprints. For the PSD analysis, the features vector, for each single epoch, was composed of the 272 entries representing the relative power (extracted using the Welch method) of alpha (8 - 13 Hz) and beta (13 - 30 Hz) frequency bands, separately for each of the 68 regions of interest. For the PLV analysis, the features vector, for each single epoch and for each frequency band, was composed of 2,278 entries representing the connectivity profile (upper triangular of the connectivity matrix), where each entry was computed as:

$$PLV_{xy} = \frac{1}{T} \left| \sum_{t=1}^T e^{-i(\varphi x(t) - \varphi y(t))} \right|$$

where T is the epoch length and φ is the instantaneous phase. Furthermore, we have replicated the analysis using two other connectivity metrics, the amplitude envelope correlation (AEC) approach [34] and the novel and revised version of PLV (icPLV) [35], which has been shown to be particularly valid to estimate synchronization in the presence of volume conduction or source leakage effects. For the network analysis, in order to keep a nodal resolution, we have computed the EC, a centrality measure based on the spectral decomposition of the weighted connectivity matrix [30]. The EC was computed using the Brain Connectivity Toolbox (brain-connectivity-toolbox.net) [31]. In this latter case the features vector, for each single epoch and separately for each frequency band, was composed of 68 entries, each representing the centrality value of the corresponding ROI. As a final step, in order to estimate the

similarity among each pairs of possible observations (between-epochs), we computed the Euclidian distance between features vectors (individual profiles) independently for PSD, PLV and EC analysis, thus obtaining, for each analysis, a square and symmetric matrix of distances, with the dimension equals to (number of subjects) * (number of sessions) * (number of tasks) * (number of epochs) as shown in Figure 1. From this distances matrix, we have computed the average distances across epochs for each of the following six scenarios: (i) within-task, within-session and within-subject; (ii) between-tasks, within-session and within-subject; (iii) between-sessions, within-task and within-subject; (iv) between-sessions, between-tasks and within-subject; (v) within-task, within-session and between-subjects; (vi) all-between. All the code, developed in Matlab, reporting the extraction of the profiles and their comparison, is freely available at the following link in Github: <https://github.com/matteogithub/individuality>.

2.5 Statistical analysis

The statistical analysis was performed by using the non-parametric Kruskal-Wallis test [32] followed by two-stage linear step-up procedure of Benjamini, Krieger and Yekutieli [33] to account for the multiple comparison problem.

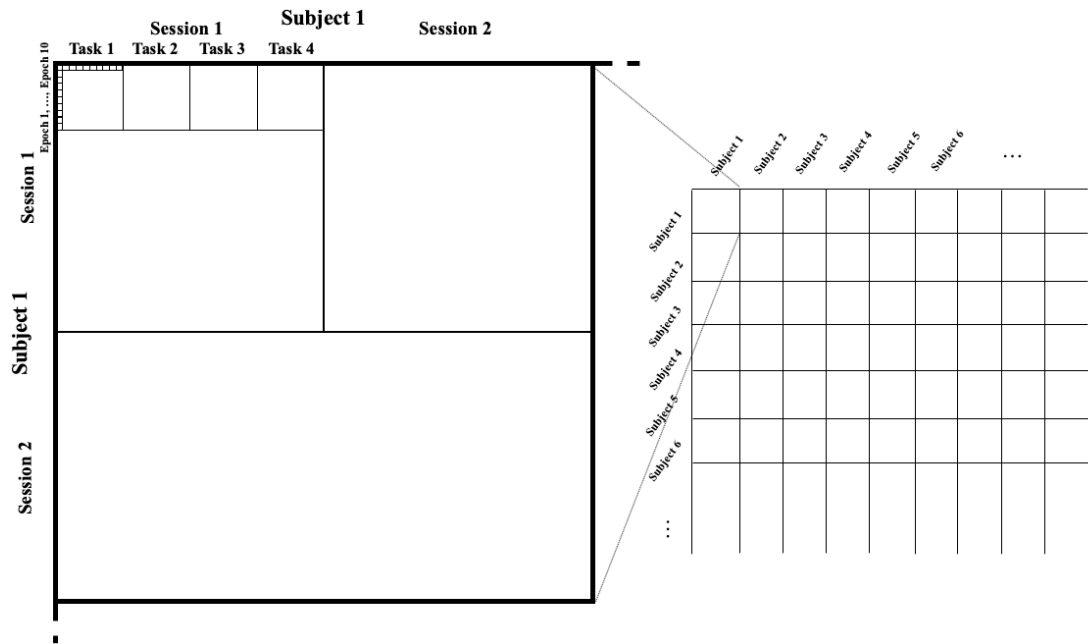


Figure 1. A schematic representation of the first block (one subject) of the matrix containing the distances for all the possible investigated scenarios.

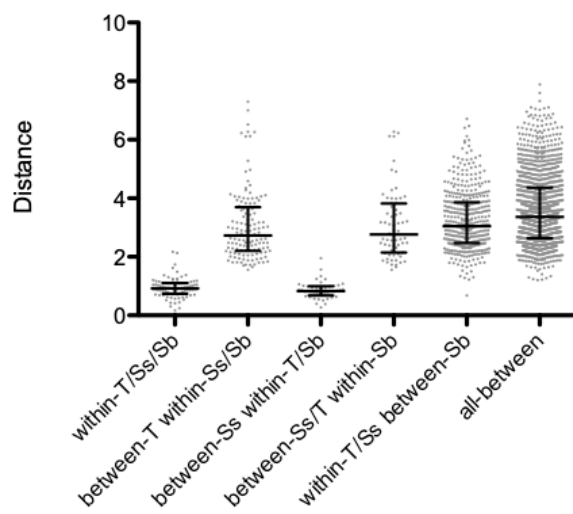


Figure 2. Scatterplot of distances obtained by using the PSD approach. Bars represent median and interquartile range. T is for task, Ss for session and Sb for subject.

TABLE I

STATISTICAL RESULTS FOR PSD ANALYSIS

	Mean rank diff.	p-value
w-T/Ss/Sb vs. b-T w-Ss/Sb	-873.129	<0.0001
w-T/Ss/Sb vs. b-Ss w-T/Sb	14.6023	0.9056
w-T/Ss/Sb vs. b-Ss/T w-Sb	-907.163	<0.0001
w-T/Ss/Sb vs. w-T/Ss b-Sb	-1033.61	<0.0001
w-T/Ss/Sb vs. all-b	-1209.25	<0.0001
b-T w-Ss/Sb vs. b-Ss w-T/Sb	887.731	<0.0001
b-T w-Ss/Sb vs. b-Ss/T w-Sb	-34.0341	0.7350
b-T w-Ss/Sb vs. w-T/Ss b-Sb	-160.484	0.0153
b-T w-Ss/Sb vs. all-b	-336.122	<0.0001
b-Ss w-T/Sb vs. b-Ss/T w-Sb	-921.765	<0.0001
b-Ss w-T/Sb vs. w-T/Ss b-Sb	-1048.21	<0.0001
b-Ss w-T/Sb vs. all-b	-1223.85	<0.0001
b-Ss/T w-Sb vs. w-T/Ss b-Sb	-126.450	0.1509
b-Ss/T w-Sb vs. all-b	-302.088	0.0003
w-T/Ss b-Sb vs. all-b	-175.638	<0.0001

Statistics refer to non-parametric multiple comparison tests (on mean rank) using the FDR correction approach, where w- and b- refer to within and between scenarios respectively. T, Ss and Sb refer to task, session and subject.

3. Results

3.1 PSD

Results derived from PSD analysis are shown in Figure 2 and the corresponding statistics are summarized in Table 1. The lower distances were observed for the within-task, within-session, within-subject scenario (0.95 ± 0.34) and for the between-sessions, within-task, within-subject scenario (0.87 ± 0.30). The distances increased for the between-tasks scenarios, both for within-session (3.06 ± 1.20) and for between-sessions (3.09 ± 1.19). The distances further increased for the between-subjects' scenarios, both for within-session, within-task (3.23 ± 1.00) and for all between (3.59 ± 1.18). Values represent mean and standard deviation.

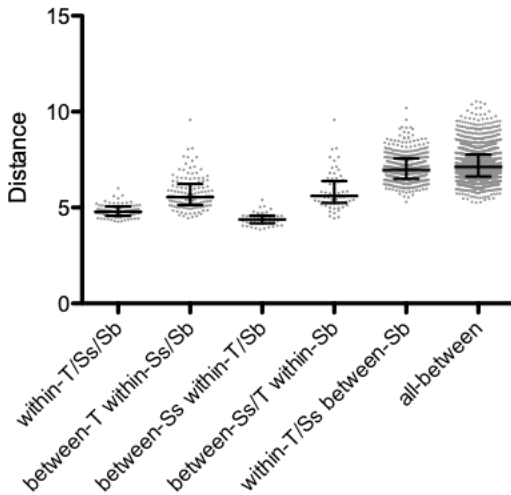


Figure 3. Scatterplot of beta band distances obtained by using the PLV connectivity approach. Bars represent median and interquartile range. T is for task, Ss for session and Sb for subject.

TABLE II

STATISTICAL RESULTS FOR PLV BETA BAND

	Mean rank diff.	p-value
w-T/Ss/Sb vs. b-T w-Ss/Sb	-317.8	0.0005
w-T/Ss/Sb vs. b-Ss w-T/Sb	61.03	0.6202
w-T/Ss/Sb vs. b-Ss/T w-Sb	-382.5	0.0004
w-T/Ss/Sb vs. w-T/Ss b-Sb	-1104	<0.0001
w-T/Ss/Sb vs. all-b	-1217	<0.0001
b-T w-Ss/Sb vs. b-Ss w-T/Sb	378.8	0.0011
b-T w-Ss/Sb vs. b-Ss/T w-Sb	-64.72	0.5198
b-T w-Ss/Sb vs. w-T/Ss b-Sb	-786.1	<0.0001
b-T w-Ss/Sb vs. all-b	-899.3	<0.0001
b-Ss w-T/Sb vs. b-Ss/T w-Sb	-443.6	0.0006
b-Ss w-T/Sb vs. w-T/Ss b-Sb	-1165	<0.0001
b-Ss w-T/Sb vs. all-b	-1278	<0.0001
b-Ss/T w-Sb vs. w-T/Ss b-Sb	-721.4	<0.0001
b-Ss/T w-Sb vs. all-b	-834.6	<0.0001
w-T/Ss b-Sb vs. all-b	-113.1	0.0017

Statistics refer to non-parametric multiple comparison tests (on mean rank) using the FDR correction approach, where w- and b- refers to within and between scenarios respectively. T, Ss and Sb refer to task, session and subject.

3.2 Connectivity

Results derived from PLV based analysis in the beta band are consistent with those obtained by PSD as shown in Figure 3 and the corresponding statistics summarized in Table 2. Again, the lower distances were observed for the within-task, within-session, within -subject scenario (4.82 ± 0.33) and for the between-sessions, within-task, within-subject scenario (4.40 ± 0.34). The distances increased for the between-tasks scenarios, both for within-session (5.74 ± 0.85) and for between-sessions (5.85 ± 0.96). Finally, the distances further increased for the between-subjects' scenarios, both for within-session, within-task (7.07 ± 0.76) and for all between (7.25 ± 0.87).

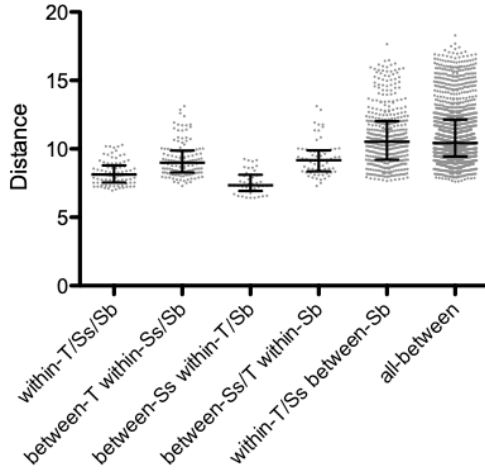


Figure 4. Scatterplot of alpha band distances obtained by using the PLV connectivity approach. Bars represent median and interquartile range. T is for task, Ss for session and Sb for subject.

TABLE III

STATISTICAL RESULTS FOR PLV ALPHA BAND

	Mean rank diff.	p-value
w-T/Ss/Sb vs. b-T w-Ss/Sb	-356.220	0.0001
w-T/Ss/Sb vs. b-Ss w-T/Sb	165.750	0.1783
w-T/Ss/Sb vs. b-Ss/T w-Sb	-402.515	0.0002
w-T/Ss/Sb vs. w-T/Ss b-Sb	-933.130	<0.0001
w-T/Ss/Sb vs. all-b	-974.344	<0.0001
b-T w-Ss/Sb vs. b-Ss w-T/Sb	521.970	<0.0001
b-T w-Ss/Sb vs. b-Ss/T w-Sb	-46.2955	0.6452
b-T w-Ss/Sb vs. w-T/Ss b-Sb	-576.910	<0.0001
b-T w-Ss/Sb vs. all-b	-618.124	<0.0001
b-Ss w-T/Sb vs. b-Ss/T w-Sb	-568.265	<0.0001
b-Ss w-T/Sb vs. w-T/Ss b-Sb	-1098.88	<0.0001
b-Ss w-T/Sb vs. all-b	-1140.09	<0.0001
b-Ss/T w-Sb vs. w-T/Ss b-Sb	-530.614	<0.0001
b-Ss/T w-Sb vs. all-b	-571.828	<0.0001
w-T/Ss b-Sb vs. all-b	-41.2140	0.2530

Statistics refer to non-parametric multiple comparison tests (on mean rank) using the FDR correction approach, where w- and b- refer to within and between scenarios respectively. T, Ss and Sb refer to task, session and subject.

The results show a similar pattern, still slightly less marked, also for the alpha band as shown in Figure 4 and the corresponding statistics summarized in Table 3. In this case, again the lower distances were observed for the within-task, within-session, within-subject scenario (8.25 ± 0.86) and for the between-sessions, within-task, within-subject scenario (7.55 ± 0.83). The distances increased for between-tasks scenarios, both for within-session (9.21 ± 1.26) and for between-sessions (9.32 ± 1.27). Finally, the distances further increased for the between-subjects' scenarios, both for within-session, within-task (10.86 ± 2.11) and for all between (11.01 ± 2.16). In order to give a more detailed description of the connectivity patterns obtained during the different tasks and the different sessions, we have represented the corresponding average (the average was computed over epochs and subjects) matrices in Figure 5.

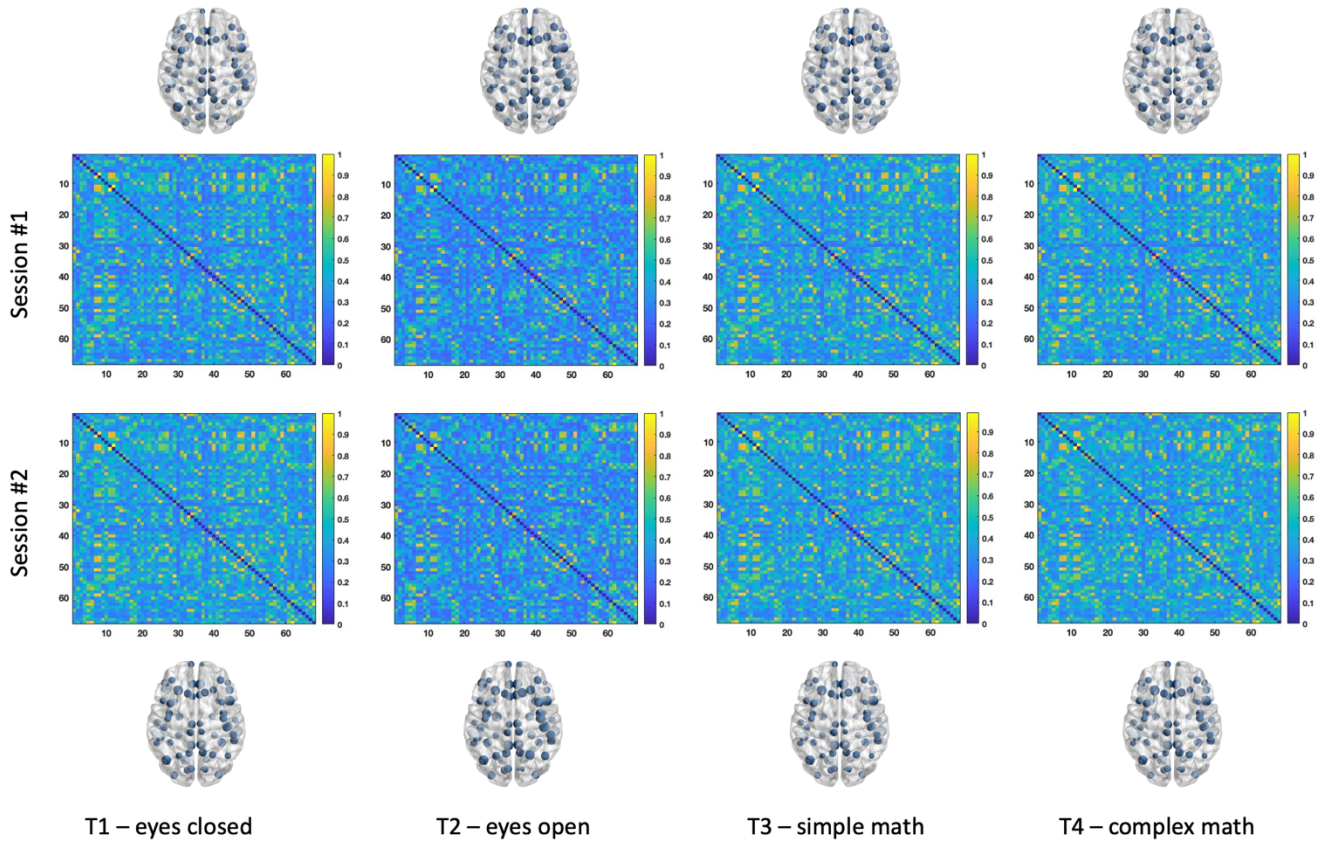


Figure 5. Average connectivity matrices and glass brains visualization computed using PLV methods in alpha band for each task and for both sessions.

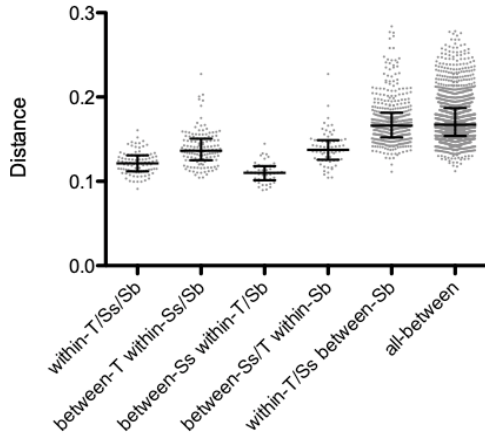


Figure 6. Scatterplot of alpha band distances obtained by using the PLV connectivity approach and eigenvector centrality. Bars represent median and interquartile range. T is for task, Ss for session and Sb for subject.

TABLE IV

STATISTICAL RESULTS FOR EIGENVECTOR CENTRALITY

	Mean rank diff.	p-value
w-T/Ss/Sb vs. b-T w-Ss/Sb	-309.489	0.0007
w-T/Ss/Sb vs. b-Ss w-T/Sb	93.5795	0.4473
w-T/Ss/Sb vs. b-Ss/T w-Sb	-307.186	0.0047
w-T/Ss/Sb vs. w-T/Ss b-Sb	-1084.05	<0.0001
w-T/Ss/Sb vs. all-b	-1134.76	<0.0001
b-T w-Ss/Sb vs. b-Ss w-T/Sb	403.068	0.0005
b-T w-Ss/Sb vs. b-Ss/T w-Sb	2.30303	0.9817
b-T w-Ss/Sb vs. w-T/Ss b-Sb	-774.561	<0.0001
b-T w-Ss/Sb vs. all-b	-825.269	<0.0001
b-Ss w-T/Sb vs. b-Ss/T w-Sb	-400.765	0.0020
b-Ss w-T/Sb vs. w-T/Ss b-Sb	-1177.63	<0.0001
b-Ss w-T/Sb vs. all-b	-1228.34	<0.0001
b-Ss/T w-Sb vs. w-T/Ss b-Sb	-776.864	<0.0001
b-Ss/T w-Sb vs. all-b	-827.573	<0.0001
w-T/Ss b-Sb vs. all-b	-50.7081	0.1596

Statistics refer to non-parametric multiple comparison tests (on mean rank) using the FDR correction approach, where w- and b- refer to within and between scenarios respectively. T, Ss and Sb refer to task, session and subject.

3.3 Network centrality

Results derived from the application of EC on PLV based analysis (in the beta band) are still consistent with the previous reports, as shown in Figure 6 and the corresponding statistics summarized in Table 4. Again, the lower distances were observed for the within-task, within-session, within-subject scenario (0.12 ± 0.01) and for the between-sessions, within-task, within-subject scenario (0.11 ± 0.01). The distances increased for the between-tasks scenarios, both for within-session (0.14 ± 0.02) and for between-sessions (0.14 ± 0.02). Finally, the distances further increased for the between-subjects' scenarios, both for within-session, within-task (0.17 ± 0.03) and for all between (0.17 ± 0.03). In the Supplementary material we have also reported the results derived from the application of a very common technique used to threshold the connectivity matrix, namely the MST, on the EC based on PLV.

3.4 Between-tasks comparison

In order to understand if the reported between-tasks increase of distances comes from some specific task-switching (i.e., cognitive effort or eyes-closed/eyes-open) we further investigate this issue for both PSD and PLV beta band. For the PSD analysis, as shown in Figure 7 the increase of distance in the between-tasks scenario mainly comes from the comparison of eyes-closed resting-state (T1) with the eyes-closed complex mathematical task (T4) and from the comparison of simple mathematical task (T3) with the eyes-closed complex mathematical task (T4). The main effect was tested using the Kruskal-Wallis approach obtaining a χ^2 equals 27.2 to and p-value $< .0001$. For the PLV beta band analysis, as shown in Figure 8 the increase of distance in the between-tasks scenario mainly comes from the comparison of eyes-open resting-state (T2) with the eyes-closed complex mathematical task (T4). The main effect was tested using the Kruskal-Wallis approach obtaining a χ^2 equals 17.6 to and p-value equals to 0.004. All these analyses were performed in the within-session and within-subject scenario.

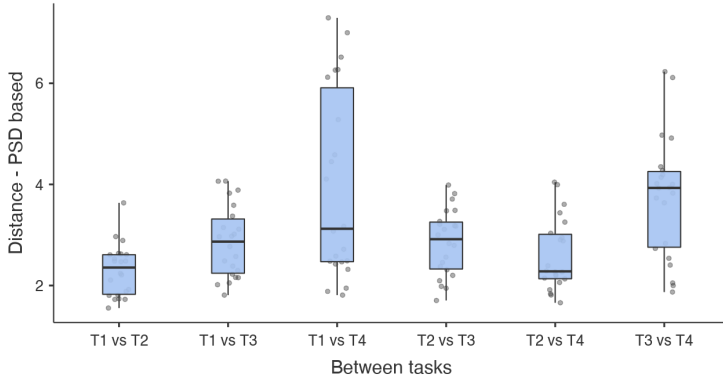


Figure 7. Between task comparisons for PSD analysis. T1 refers to eyes-closed resting-state, T2 to eyes-open resting-state, T3 to eyes-closed simple mathematical task and T4 to eyes-closed complex mathematical task. Bars represent media and interquartile range.

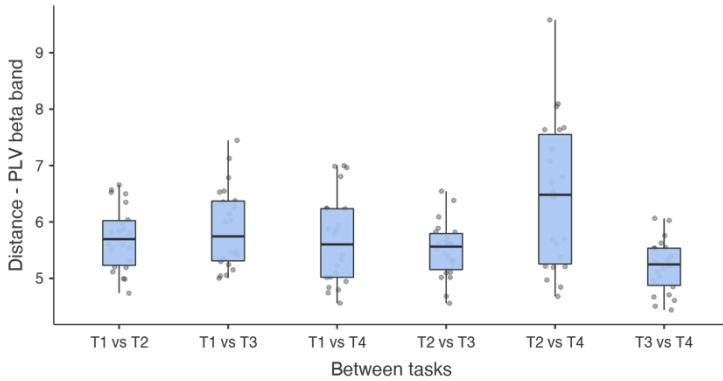


Figure 8. Between task comparisons for PLV beta band analysis. T1 refers to eyes-closed resting-state, T2 to eyes-open resting-state, T3 to eyes-closed simple mathematical task and T4 to eyes-closed complex mathematical task. Bars represent media and interquartile range.

3.5 The effect of the connectivity metric

Although a comprehensive and detailed comparison among different connectivity metrics is out of the scope of the present study, in order to investigate the effect of the arbitrary choice of connectivity metric we have replicated part of the analysis to understand if the reported results still hold when a different method to estimate the connectivity is applied. In this context, here we report the results obtained using the amplitude envelope correlation (AEC) approach [34] and the novel and revised version of PLV

(icPLV) [35], which has been shown to be particularly valid to estimate synchronization in the presence of volume conduction or source leakage effects. The results obtained by using these two different approaches are reported in Figure 9 and Figure 10 respectively for the AEC and icPLV approaches.

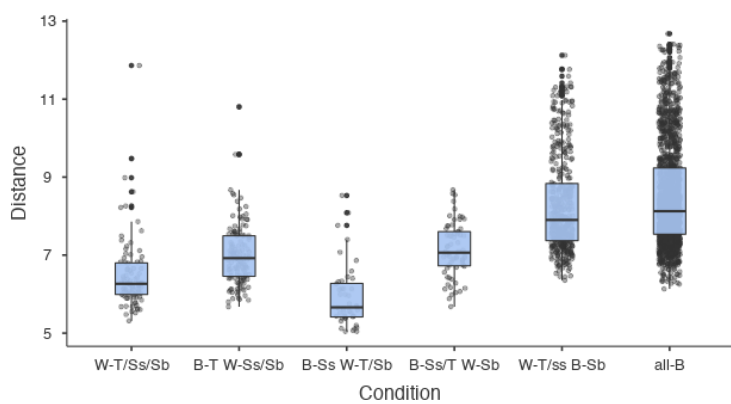


Figure 9. Scatterplot of beta band distances obtained by using the AEC connectivity approach. Bars represent median and interquartile range.

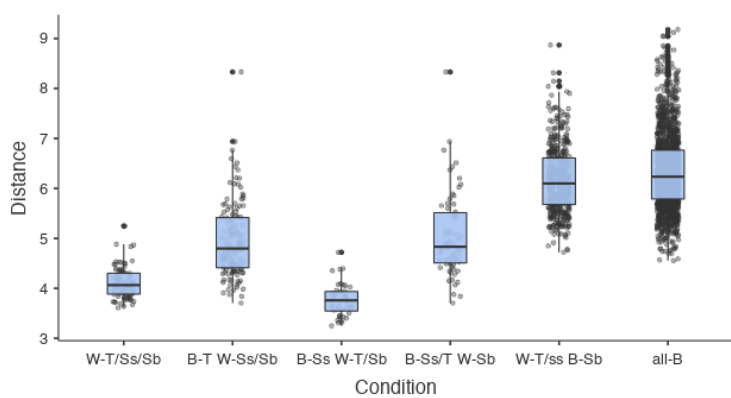


Figure 10. Scatterplot of beta band distances obtained by using the icPLV connectivity approach. Bars represent median and interquartile range.

3.6 The effect of different atlas

In this section we report the results obtained using a different atlas, namely Schaefer atlas with 17 networks as described in [28], for the PSD (see Figure 11), PLV (see Figure 12) and EC PLV-based

metrics (see Figure 13). For all the three different analyses, the corresponding findings are in line with those obtained using the Desikan-Killiany atlas.

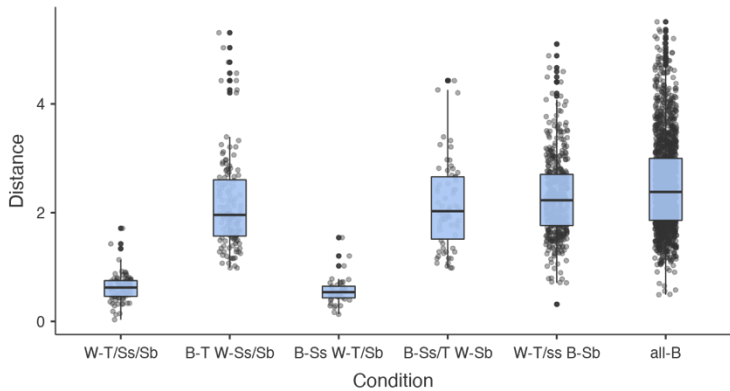


Figure 11. Scatterplot of distances obtained by using the PSD approach with the Schaefer atlas. Bars represent median and interquartile range. T is for task, Ss for session and Sb for subject.

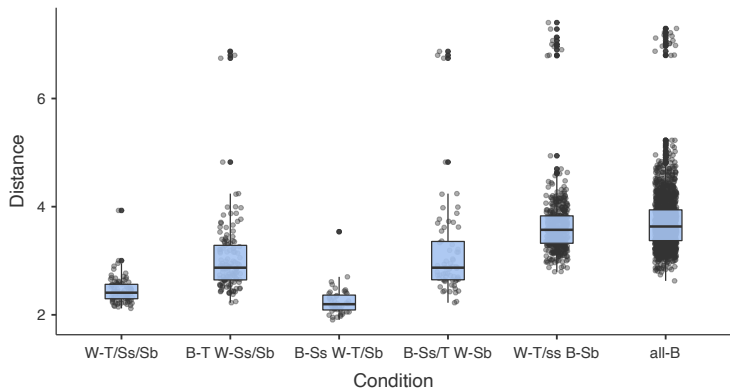


Figure 12. Scatterplot of distances obtained by using the PLV approach with the Schaefer atlas in beta band. Bars represent median and interquartile range. T is for task, Ss for session and Sb for subject.

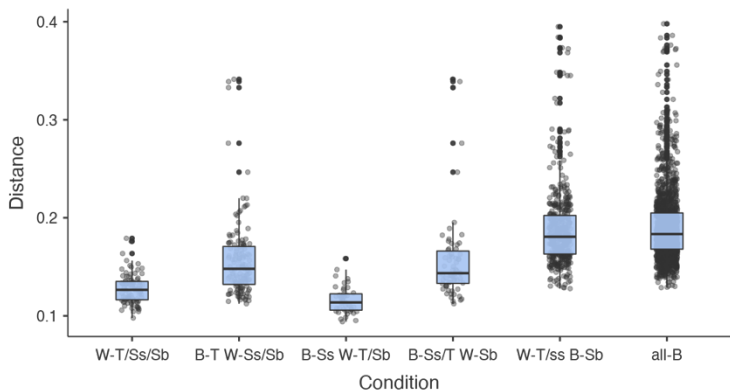


Figure 13. Scatterplot of distances obtained by using the EC PLV-based approach with the Schaefer atlas in beta band. Bars represent median and interquartile range. T is for task, Ss for session and Sb for subject.

3.7 The effect of time window

Although the original epoch length was defined accordingly to a previous work which evaluated the effect of epoch length on connectivity and network metrics, in this section we report the results obtained using different time windows on beta band PLV connectivity profiles. In particular, in Figure 14 it is represented the variability of the reported effects on three different epoch length, respectively 6 s (as the main finding), 2 s and 1 s. Although the main effects are still visible the intra task condition variability (see interquartile ranges) looks to increase as the epoch length decrease.

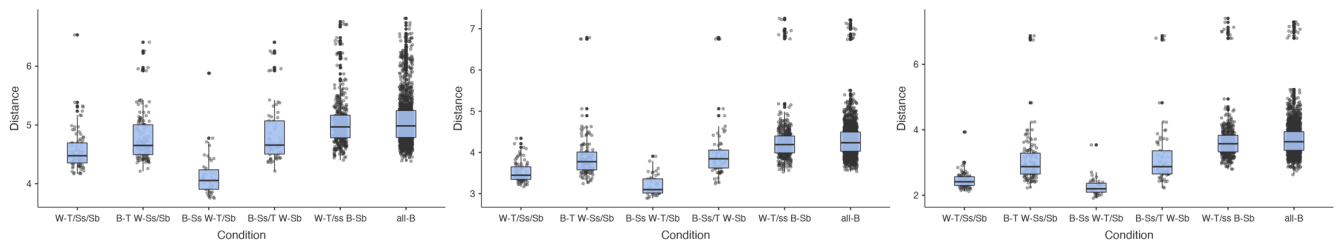


Figure 14. Scatterplot of distances obtained by using the PLV approach with three different epoch lengths: 1 second (left panel), 2 seconds (middle panel) and 6 seconds (right panel). Bars represent median and interquartile range. T is for task, Ss for session and Sb for subject.

4. Discussion and conclusions

In summary, in this work we aimed to investigate how the variability due to subject, session and task affects EEG power, connectivity and network features estimated using source-reconstructed EEG time-series. Although this question was extensively investigated using fMRI [2], [6], [14], high density EEG, which still represents a very important and useful clinical tool, has received less attention in this context. Although, numerous studies have investigated the possibility to use EEG signals to develop biometric systems, only recently more attention was devoted to the study of subject variability and stability over-time and states [15].

The results of this study show three main relevant points. First, as expected, for all the different analyses, PSD, PLV and EC based approaches, the lower distances were observed in the scenario corresponding to a simple between epochs scheme, within the same subject, the same session and the same task. It should be highlighted that this also represents the more common scenario in which studies do not consider the variance induced by subject-specific features, multi-sessions and/or by multi-tasks setup. Second, probably the more interesting finding, the distances obtained using the between-sessions, within-task, within-subject scenario are comparable with the previous one (namely, within-session scenario) for all the performed analyses. This finding suggests that the variance due to the session may be considered negligible, but we need to highlight that the task design is not considering the possible effects due to learning process or memory recall/consolidation processes. Third, conversely, the effect due to the task (task-switching) is substantial, as also highlighted by the statistics and consistent for all the different analyses (i.e., PSD, PLV in beta and alpha bands and EC analysis). Finally, as expected, the distances strongly increase in the between-subjects scenario, showing a clear effect due to specific subject, thus confirming the importance to address the issue related with the variance within a group.

The reported results support, as recently reported using a scalp-level EEG analysis [15], the existence of well-defined subject-specific profiles and that these features may be considered stable over a defined and limited time range. These results are also in line with the fact that task-invariant subject-specific features are stronger than task-dependent group profiles. Moreover, as reported in the between-tasks effect, it seems that the reported increase of distance in this scenario is not merely due to eyes-closed and eyes-open switching. It is interesting to highlight, that the present findings, derived from source-reconstructed EEG time-series, are also in line with previous outcomes derived from fMRI network analysis. In particular, recently Finn et al. [3] have reported that brain functional organization varies between individuals, that this variability is robust and reliable and that can be used to identify subjects from a large

group. Moreover, the authors also report that identification is successful across scan sessions and even between task and rest conditions. Later, Gratton et al. [14] have reported that functional networks, as measured by fMRI, are dominated by common organizational principles and stable individual features, with more modest contributions from task-state and day-to-day variability. We also would like to highlight that our results are based on a very limited set of tasks and therefore are not easily generalizable. We are aware that the reported findings would need to be replicated in set of EEG recordings that include a large number of subjects and tasks.

Although it is not possible to directly compare the absolute distances derived from the different features to understand if any approach outperforms the others, it is worth to highlight that the PSD analysis seems to be the most sensitive approach to inter-condition variability as marked by the larger mean rank differences for all the different scenarios investigated. This latest finding may suggest using this very simple and easily interpretable approach to check for the stability over session and task of the EEG signals.

Finally, the reported findings (derived from source level analysis) are in line with the results previously reported at scalp level [10], [13]. On the other hand, these results also confirm what is generally observable by designing a brain computer interface system. In fact, even though it is still remarkable a strong effect of task-switching, it is still evident that the individual properties may strongly hinder the generalization of the approach (failing to keep a good performance across different subjects). It is also of relevance to notice that the results reported using the PLV approach have been confirmed when the analysis was replicated using two other connectivity metrics, namely AEC and icPLV. In particular, the findings related to this last metric (icPLV), which has been shown to be particularly valid to estimate synchronization in the presence of volume conduction or source leakage effects [35], suggest that the reported effects are not a consequence of possible bias in estimating EEG connectivity. As reported, the results obtained on PSD, PLV and EC still hold when a different parcellation scheme [28] was used for the analysis.

In light of what we have shown up to this point, in our opinion, future studies should investigate how connectivity and network similarity across multiple tasks and sessions varies between different clinical conditions and, in particular it would be of relevance to evaluate its association with behavior.

In conclusion, we have shown that source-level EEG analysis confirms that PSD, PLV and PLV derived functional brain network, as measured by nodal centrality (namely, eigenvector centrality), are stable over-time, dominated by individual properties but largely dependent from the specific task. These findings

may have important implications for both clinical (e.g., biomarkers) and bio-engineering applications (e.g., biometric systems and brain computer interfaces).

References

- [1] O. Miranda-Dominguez *et al.*, “Connectotyping: Model Based Fingerprinting of the Functional Connectome,” *PLOS ONE*, vol. 9, no. 11, p. e111048, Nov. 2014, doi: 10.1371/journal.pone.0111048.
- [2] E. S. Finn *et al.*, “Functional connectome fingerprinting: identifying individuals using patterns of brain connectivity,” *Nature Neuroscience*, vol. 18, no. 11, pp. 1664–1671, Nov. 2015, doi: 10.1038/nn.4135.
- [3] E. S. Finn and R. Todd Constable, “Individual variation in functional brain connectivity: implications for personalized approaches to psychiatric disease,” *Dialogues Clin Neurosci*, vol. 18, no. 3, pp. 277–287, Sep. 2016.
- [4] M. Arns, “EEG-Based Personalized Medicine in ADHD: Individual Alpha Peak Frequency as an Endophenotype Associated with Nonresponse,” *Journal of Neurotherapy*, vol. 16, no. 2, pp. 123–141, Apr. 2012, doi: 10.1080/10874208.2012.677664.
- [5] C. Horien, X. Shen, D. Scheinost, and R. T. Constable, “The individual functional connectome is unique and stable over months to years,” *NeuroImage*, vol. 189, pp. 676–687, Apr. 2019, doi: 10.1016/j.neuroimage.2019.02.002.
- [6] O. Miranda-Dominguez, E. Feczko, D. S. Grayson, H. Walum, J. T. Nigg, and D. A. Fair, “Heritability of the human connectome: A connectotyping study,” *Network Neuroscience*, vol. 2, no. 2, pp. 175–199, Nov. 2017, doi: 10.1162/netn_a_00029.
- [7] M. Demuru *et al.*, “Functional and effective whole brain connectivity using magnetoencephalography to identify monozygotic twin pairs,” *Scientific Reports*, vol. 7, no. 1, p. 9685, Aug. 2017, doi: 10.1038/s41598-017-10235-y.
- [8] M. DelPozo-Banos, C. M. Travieso, C. T. Weidemann, and J. B. Alonso, “EEG biometric identification: a thorough exploration of the time-frequency domain,” *J Neural Eng*, vol. 12, no. 5, p. 056019, Oct. 2015, doi: 10.1088/1741-2560/12/5/056019.
- [9] M. Fraschini, A. Hillebrand, M. Demuru, L. Didaci, and G. L. Marcialis, “An EEG-Based Biometric System Using Eigenvector Centrality in Resting State Brain Networks,” *IEEE Signal Processing Letters*, vol. 22, no. 6, pp. 666–670, Jun. 2015, doi: 10.1109/LSP.2014.2367091.
- [10] D. L. Rocca *et al.*, “Human Brain Distinctiveness Based on EEG Spectral Coherence Connectivity,” *IEEE Transactions on Biomedical Engineering*, vol. 61, no. 9, pp. 2406–2412, Sep. 2014, doi: 10.1109/TBME.2014.2317881.
- [11] A. Crobe, M. Demuru, L. Didaci, G. L. Marcialis, and M. Fraschini, “Minimum spanning tree and k-core decomposition as measure of subject-specific EEG traits,” *Biomed. Phys. Eng. Express*, vol. 2, no. 1, p. 017001, Jan. 2016, doi: 10.1088/2057-1976/2/1/017001.
- [12] S. Barra, A. Casanova, M. Fraschini, and M. Nappi, “Fusion of physiological measures for multimodal biometric systems,” *Multimed Tools Appl*, vol. 76, no. 4, pp. 4835–4847, Feb. 2017, doi: 10.1007/s11042-016-3796-1.
- [13] M. Fraschini, S. M. Pani, L. Didaci, and G. L. Marcialis, “Robustness of functional connectivity metrics for EEG-based personal identification over task-induced intra-class and inter-class variations,” *Pattern Recognition Letters*, vol. 125, pp. 49–54, Jul. 2019, doi: 10.1016/j.patrec.2019.03.025.
- [14] C. Gratton *et al.*, “Functional Brain Networks Are Dominated by Stable Group and Individual Factors, Not Cognitive or Daily Variation,” *Neuron*, vol. 98, no. 2, pp. 439–452.e5, Apr. 2018, doi: 10.1016/j.neuron.2018.03.035.
- [15] R. Cox, A. C. Schapiro, and R. Stickgold, “Variability and stability of large-scale cortical oscillation patterns,” *Network Neuroscience*, vol. 2, no. 4, pp. 481–512, Feb. 2018, doi: 10.1162/netn_a_00046.
- [16] M. Lai, M. Demuru, A. Hillebrand, and M. Fraschini, “A comparison between scalp- and source-reconstructed EEG networks,” *Scientific Reports*, vol. 8, no. 1, p. 12269, Aug. 2018, doi: 10.1038/s41598-018-30869-w.
- [17] J.-P. Lachaux, E. Rodriguez, J. Martinerie, and F. J. Varela, “Measuring phase synchrony in brain signals,” *Human Brain Mapping*, vol. 8, no. 4, pp. 194–208, Jan. 1999, doi: 10.1002/(SICI)1097-0193(1999)8:4<194::AID-HBM4>3.0.CO;2-C.
- [18] M. S. Hämmäläinen and R. J. Ilmoniemi, “Interpreting magnetic fields of the brain: minimum norm estimates,” *Med. Biol. Eng. Comput.*, vol. 32, no. 1, pp. 35–42, Jan. 1994, doi: 10.1007/BF02512476.
- [19] M. Hassan, O. Dufor, I. Merlet, C. Berrou, and F. Wendling, “EEG Source Connectivity Analysis: From Dense Array Recordings to Brain Networks,” *PLoS One*, vol. 9, no. 8, Aug. 2014, doi: 10.1371/journal.pone.0105041.
- [20] M. Demuru, S. M. L. Cava, S. M. Pani, and M. Fraschini, “A comparison between power spectral density and network metrics: an EEG study,” Apr. 2019.
- [21] A. Delorme and S. Makeig, “EEGLAB: an open source toolbox for analysis of single-trial EEG dynamics including independent component analysis,” *J. Neurosci. Methods*, vol. 134, no. 1, pp. 9–21, Mar. 2004, doi: 10.1016/j.jneumeth.2003.10.009.
- [22] F. Tadel, S. Baillet, J. C. Mosher, D. Pantazis, and R. M. Leahy, “Brainstorm: a user-friendly application for MEG/EEG analysis,” *Comput Intell Neurosci*, vol. 2011, p. 879716, 2011, doi: 10.1155/2011/879716.
- [23] A. Gramfort, T. Papadopoulos, E. Olivi, and M. Clerc, “OpenMEEG: opensource software for quasistatic bioelectromagnetics,” *Biomed Eng Online*, vol. 9, p. 45, Sep. 2010, doi: 10.1186/1475-925X-9-45.

- [24] S. Cutini, P. Scatturin, and M. Zorzi, “A new method based on ICBM152 head surface for probe placement in multichannel fNIRS,” *NeuroImage*, vol. 54, no. 2, pp. 919–927, Jan. 2011, doi: 10.1016/j.neuroimage.2010.09.030.
- [25] L. Douw, D. Nieboer, C. J. Stam, P. Tewarie, and A. Hillebrand, “Consistency of magnetoencephalographic functional connectivity and network reconstruction using a template versus native MRI for co-registration,” *Human Brain Mapping*, vol. 39, no. 1, pp. 104–119, Jan. 2018, doi: 10.1002/hbm.23827.
- [26] F.-H. Lin, T. Witzel, S. P. Ahlfors, S. M. Stufflebeam, J. W. Belliveau, and M. S. Hämäläinen, “Assessing and improving the spatial accuracy in MEG source localization by depth-weighted minimum-norm estimates,” *NeuroImage*, vol. 31, no. 1, pp. 160–171, May 2006, doi: 10.1016/j.neuroimage.2005.11.054.
- [27] R. S. Desikan *et al.*, “An automated labeling system for subdividing the human cerebral cortex on MRI scans into gyral based regions of interest,” *NeuroImage*, vol. 31, no. 3, pp. 968–980, Jul. 2006, doi: 10.1016/j.neuroimage.2006.01.021.
- [28] A. Schaefer *et al.*, “Local-Global Parcellation of the Human Cerebral Cortex from Intrinsic Functional Connectivity MRI,” *Cereb. Cortex*, vol. 28, no. 9, pp. 3095–3114, 01 2018, doi: 10.1093/cercor/bhx179.
- [29] M. Fraschini, M. Demuru, A. Crobe, F. Marrosu, C. J. Stam, and A. Hillebrand, “The effect of epoch length on estimated EEG functional connectivity and brain network organisation,” *J Neural Eng*, vol. 13, no. 3, p. 036015, 2016, doi: 10.1088/1741-2560/13/3/036015.
- [30] B. Ruhnau, “Eigenvector-centrality — a node-centrality?,” *Social Networks*, vol. 22, no. 4, pp. 357–365, Oct. 2000, doi: 10.1016/S0378-8733(00)00031-9.
- [31] M. Rubinov and O. Sporns, “Complex network measures of brain connectivity: Uses and interpretations,” *NeuroImage*, vol. 52, no. 3, pp. 1059–1069, Sep. 2010, doi: 10.1016/j.neuroimage.2009.10.003.
- [32] W. H. Kruskal and W. A. Wallis, “Use of Ranks in One-Criterion Variance Analysis,” *Journal of the American Statistical Association*, vol. 47, no. 260, pp. 583–621, Dec. 1952, doi: 10.1080/01621459.1952.10483441.
- [33] Y. Benjamini, A. M. Krieger, and D. Yekutieli, “Adaptive linear step-up procedures that control the false discovery rate,” *Biometrika*, vol. 93, no. 3, pp. 491–507, Sep. 2006, doi: 10.1093/biomet/93.3.491.
- [34] J. F. Hipp, D. J. Hawellek, M. Corbetta, M. Siegel, and A. K. Engel, “Large-scale cortical correlation structure of spontaneous oscillatory activity,” *Nature Neuroscience*, vol. 15, no. 6, pp. 884–890, Jun. 2012, doi: 10.1038/nn.3101.
- [35] R. Bruña, F. Maestú, and E. Pereda, “Phase locking value revisited: teaching new tricks to an old dog,” *J Neural Eng*, vol. 15, no. 5, p. 056011, Oct. 2018, doi: 10.1088/1741-2552/aacfe4.